

## Carboxyl-terminal Vesicular Stomatitis Virus G Protein-tagged Intestinal Na<sup>+</sup>-dependent Glucose Cotransporter (SGLT1)

MAINTENANCE OF SURFACE EXPRESSION AND GLOBAL TRANSPORT FUNCTION WITH SELECTIVE PERTURBATION OF TRANSPORT KINETICS AND POLARIZED EXPRESSION\*

(Received for publication, December 7, 1995)

Jerrold R. Turner<sup>†§¶</sup>, Wayne I. Lencer<sup>§||</sup>, Susan Carlson<sup>†§</sup>, and James L. Madara<sup>†§</sup>

From the <sup>†</sup>Division of Gastrointestinal Pathology, Department of Pathology, Brigham and Women's Hospital and Harvard Medical School, Boston, Massachusetts 02115, the <sup>||</sup>Combined Program in Pediatric Gastroenterology and Nutrition, Children's Hospital, Boston, Massachusetts 02115, and the <sup>§</sup>Harvard Digestive Disease Center, Boston, Massachusetts 02115

The Na<sup>+</sup>-dependent glucose transporter (SGLT1) mediates absorption of luminal glucose by the intestine. However, available intestinal cell lines that recapitulate a monolayer phenotype only express SGLT1 at low levels. Thus, to facilitate studies of the biology of SGLT1 function in epithelial monolayers, we engineered an epitope-tagged construct containing the YTDIEMNR-LGK sequence (from the vesicular stomatitis virus G protein). The tag was placed at the carboxyl terminus since this is the least conserved portion of SGLT1. Transiently transfected COS-1 cells demonstrated surface expression of the immunoreactive protein and enhanced Na<sup>+</sup>-dependent glucose uptake that was phloridzin-sensitive (a specific competitive inhibitor of SGLT1). However, subsequent detailed analyses of epitope-tagged SGLT1 using stably transfected clones derived from the Caco-2 human intestinal epithelial cell line revealed substantial effects of the epitope on critical functions of SGLT1. When compared with native SGLT1 transfectants, the apparent  $K_m$  for sugar transport was increased 23-fold (313  $\mu$ M to 7.37 mM for native *versus* epitope-tagged SGLT1). In contrast, the apparent  $K_{Na}$  for epitope-tagged SGLT1 was similar to that for native SGLT1. Permeabilization studies indicated that the C-terminal epitope tag was intracellular and thus could not directly disrupt extracellular ligand-binding sites. Immunolocalization and functional assays designed to detect polarized surface expression indicated that epitope tagging resulted in loss of apical targeting and enrichment of basolateral expression. Functional isolation of the small apical pool of epitope-tagged SGLT1 (by selective inhibition of basolateral epitope-tagged SGLT1) revealed that, despite the documented kinetic alterations in sugar transport, epitope-tagged SGLT1 could promote absorptive Na<sup>+</sup> currents. These data show that 1) the C terminus of SGLT1 is intracellular; 2) disruption of protein structure by addition of a C-termi-

nal tag leads to selective modifications of SGLT1 function; 3) the kinetics of sugar transport can be altered independently of influences on the Na<sup>+</sup>-binding site of SGLT1; and 4) the weak basolateral targeting sequence present within the epitope tag is dominant over endogenous SGLT1 apical targeting information and can direct polytopic membrane protein localization. The data also caution that subtle effects of foreign sequences must be considered when epitope tagging polytopic membrane proteins.

Our initial goal was to develop a system to study Na<sup>+</sup>-glucose transport across model intestinal epithelia. Since the ability to analyze the biology of the intestinal Na<sup>+</sup>-dependent glucose cotransporter (SGLT1) is limited by the lack of high affinity antibodies for immunochemical-based assays, we used the common approach of incorporating an exogenous epitope into SGLT1, *i.e.* epitope tagging (1). This solution has been successfully applied to analyses of nonmembranous proteins including cytoskeletal (2, 3) and cytosolic (4, 5) proteins. In contrast, membrane proteins, particularly polytopic ones with relatively rigid conformational requirements, might exhibit intolerance to epitope tagging. Such epitope tags might interfere with synthesis, folding, trafficking, and function of membrane proteins. To overcome these difficulties, the epitope tag can be placed at sites considered least likely to interfere with membrane protein function and global characteristics of the epitope-tagged construct then assayed to assure retained function. While reassuring, such assays may fail to detect subtle but critical effects on essential biologic functions. Transport proteins are ideal for assessing potential effects of epitope tagging on membrane proteins since they are precisely targeted within polarized epithelia and possess defined transport kinetics that can be measured quantitatively.

The Na<sup>+</sup>-dependent glucose transporter (SGLT1) is responsible for the bulk of intestinal glucose and Na<sup>+</sup> absorption (6–8). SGLT1 is the prototype of a family of Na<sup>+</sup>-coupled solute cotransporters, of which several homologous Na<sup>+</sup>-dependent nutrient transporters have been cloned from intestine and kidney (9). SGLT1 is apically polarized and mediates Na<sup>+</sup>-glucose cotransport across the apical membrane from the intestinal lumen. Subsequently, the basolateral GLUT2-facilitated glucose transporter and Na<sup>+</sup>-K<sup>+</sup>-ATPase mediate transport of cytoplasmic glucose and Na<sup>+</sup>, respectively, across the basolateral membrane into the interstitium (6). The resulting transepithelial transport of Na<sup>+</sup> can be recognized electrically as a trans-

\* This work was supported by National Institutes of Health Grant RO1 DK35932 and Fogarty Senior International Fellowship FO6-TWO1991 (to J. L. M.), National Institutes of Health Training Grant HL07627 and Individual National Research Service Award Grant DK09180 (to J. R. T.), National Institutes of Health Grant RO1 DK48106 (to W. I. L.), and Harvard Digestive Diseases Center Grant PO1 DK34854. The costs of publication of this article were defrayed in part by the payment of page charges. This article must therefore be hereby marked "advertisement" in accordance with 18 U.S.C. Section 1734 solely to indicate this fact.

¶ To whom correspondence should be addressed: Dept. of Pathology, Brigham and Women's Hospital, 75 Francis St., Boston, MA 02115. Tel.: 617-732-7070; Fax: 617-732-6796.

epithelial short-circuit current ( $I_{sc}$ ).<sup>1</sup> SGLT1, as originally cloned from rabbit, corresponds to a 73-kDa 662-amino acid protein with at least 11 putative transmembrane domains, an extramembranous N-terminal tail, and an extramembranous C-terminal tail (6–8). Analyses of SGLT1 in isolated brush-border vesicles or SGLT1 expression by transfected *Xenopus* oocytes indicate that cotransport involves 2 Na<sup>+</sup> ions for each sugar molecule, with a corresponding binding site  $K_m$  value of 0.11 mM (sugar) and a  $K_{Na}$  value of 32 meq/liter (10). These studies have been facilitated by the use of  $\alpha$ -methyl glucoside ( $\alpha$ MG), a selective substrate for SGLT1 that accumulates within cells, since it is neither transported by GLUT2 nor metabolized (10, 11). SGLT1-mediated sugar uptake can be specifically inhibited by phloridzin (12), thus permitting an inhibitor-based assay of function as well.

Available data indicate that the N terminus of SGLT1 is exposed cytoplasmically, but the topology of the C-terminal tail remains controversial (7–9). The N terminus of SGLT1 is highly conserved between species, and mutations in this region of SGLT1 lead to the clinical syndrome of glucose/galactose malabsorption (13–15). In contrast, the C-terminal third of SGLT1 shows the greatest interspecies diversity (9), appears to be resilient to mutation, and thus represents a potentially ideal site for epitope tagging.

To develop a system to study Na<sup>+</sup>-glucose transport across model intestinal epithelia, we employed the Caco-2 cell line. This cell line was selected since it grows as polarized monolayers, expresses and correctly sorts hydrolases to the apical membrane, and represents a model for studies of villus absorptive enterocytes, the subtype of intestinal epithelial cell responsible for nutrient absorption (16–20). Since parent Caco-2 cell lines (like other available polarized intestinal epithelial cell models) exhibit barely detectable levels of transepithelial Na<sup>+</sup>-dependent glucose transport, apparently due to an isolated deficiency of SGLT1 expression (21, 22), we sought to stably transfect Caco-2 with SGLT1. To facilitate immunochemical identification of SGLT1, we also created stable transfectants expressing an epitope-tagged SGLT1 protein. For epitope tagging, we used an 11-amino acid epitope of the vesicular stomatitis virus G protein (VSV-G) for which a well characterized monoclonal antibody is available (23). As predicted, we found that C-terminal tagging by VSV-G did not interfere with the ability of the protein to be surface-expressed or with its ability to transport substrates (Na<sup>+</sup> and glucose) and interact with specific inhibitors (phloridzin), criteria that reasonably confirm that the tagged protein functions as the native one. However, upon more detailed analyses, we found that this commonly used epitope tag both altered protein targeting and selectively influenced transport kinetics for one substrate. Nonetheless, apically expressed epitope-tagged SGLT1 was capable of generating transepithelial absorptive Na<sup>+</sup> currents. These results not only have implications regarding SGLT1 polarization, transport function, and topology-transport relationships, but also illustrate that subtle effects of an apparently successful effort at epitope tagging can disrupt biologic function. The data also illustrate critical pitfalls in the use of epitope tags in situations where protein function cannot be sensitively measured by independent means.

#### EXPERIMENTAL PROCEDURES

**Plasmid Construction**—The cDNA of rabbit intestinal SGLT1 was provided by Dr. E. Wright (UCLA) (7) and was expressed under the control of the cytomegalovirus promoter in the pCB6 eukaryotic expres-

sion vector (24). To construct SGLT1 with the VSV-G epitope tag (23) at the C terminus, bases 1996–2010 were replaced by a synthetic oligonucleotide that substituted GGG G for the stop codon. This sequence was ligated to a plasmid containing the epitope tag with a proline-rich leading sequence (GG GAG GGC CCA CCA GGC CCA TAC ACC GAC ATC GAG ATG AAC CGG CTG GGC AAG) and then ligated to the 5'-sequence using the *Mlu*I digestion site at base 1996. The complete construct was ligated into pCB6 and confirmed by direct sequencing and restriction digestion. The completed construct resulted in the addition of the sequence PRQGPPGYPYTDIEMNRLGK to the C terminus of native rabbit intestinal SGLT1.

**Cell Culture**—Cloned BBe Caco-2 cells were provided by Dr. M. Mooseker (25) and grown in high glucose Dulbecco's modified Eagle's medium (Life Technologies, Inc.) supplemented with 10% fetal calf serum and 15 mM HEPES, pH 7.4. Prior to transfection, the cells were passaged at subconfluence and replated at low density.

**Transfection**—Plasmids were purified using the QIAGEN maxiplus kit. Subconfluent Caco-2 cells plated 24 h previously were transfected using Lipofectin (Life Technologies, Inc.) in serum-free medium for 20 h. Serum was added for the subsequent 48 h, after which transfectants were selected in medium with 1.5 mg/ml G418 (Sigma). Individual clones appeared after ~4 weeks and were trypsinized individually with cloning rings. Selected clones were maintained in 0.5 mg/ml G418. These were expanded and underwent primary screening for  $\alpha$ MG uptake. Clones with high uptake underwent secondary screens based on electrophysiologic characteristics after growth on 0.33-cm<sup>2</sup> surface area Transwell supports with 0.4- $\mu$ m pores.

**Electrophysiology**—Electrophysiologic measurements were made using agar bridges and Ag-AgCl-calomel electrodes as described previously (26). Potential differences were measured before and during application of a 50- $\mu$ A current.  $I_{sc}$  and transepithelial resistance were calculated using Ohm's law.

**Sugar Uptake Assays**—Sugar (<sup>14</sup>C) $\alpha$ MG uptake assays were done using cells grown on 1-cm<sup>2</sup> surface area plastic wells. Preliminary experiments demonstrated that  $\alpha$ MG (DuPont NEN) uptake was linear from 15 min to at least 2 h. For screening assays, wells were washed three times with glucose-free HBSS and then incubated for 30 min at 37 °C with 0.2 ml of glucose-free HBSS containing 0.25  $\mu$ Ci/ml [<sup>14</sup>C] $\alpha$ MG. Wells were then washed four times with phosphate-buffered saline at 4 °C. Cells were solubilized with 0.4 ml of 0.1 N NaOH, which was added to 3.6 ml of Atomlight scintillant (DuPont NEN) and counted. For analyses of transport function, conditions were identical, except that the concentration of [<sup>14</sup>C] $\alpha$ MG was 5  $\mu$ M and unlabeled  $\alpha$ MG was added to the final concentration indicated. Specific activities were determined by counting duplicate aliquots of each solution. Duplicate samples with 0.5 mM phloridzin were included to measure non-specific  $\alpha$ MG uptake under each condition.

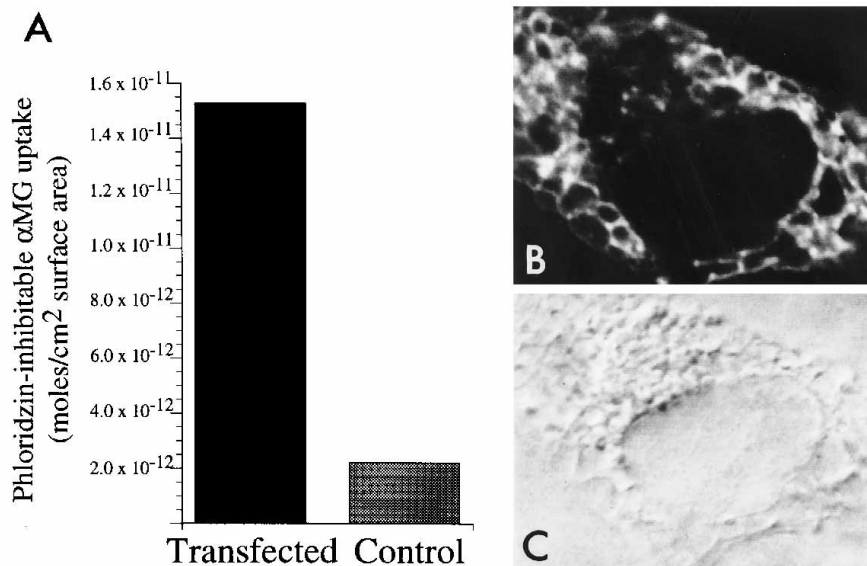
Measurement of polarized uptake in cultured monolayers was similar to that described above, but [<sup>14</sup>C] $\alpha$ MG was alternatively placed either apically or basolaterally or on both sides of the monolayer. Duplicate controls with 0.5 mM phloridzin were performed for each of these conditions, and phloridzin-inhibitable apical or basolateral uptake was calculated as a fraction of measured total uptake.

**Confocal Immunofluorescence**—For experiments comparing permeabilized with nonpermeabilized cells, Caco-2 cells transfected with epitope-tagged SGLT1 were grown on coverslips and then fixed with 3.7% (w/v) paraformaldehyde in phosphate-buffered saline. Two separate permeabilization conditions using either 0.05% Triton X-100 in phosphate-buffered saline for 1 h at room temperature or acetone for 4 min at -20 °C were used with similar results. Nonpermeabilized cells were not exposed to Triton X-100 or acetone. Cells were then immunostained for the viral epitope using mouse monoclonal antibody P5D4, kindly provided by Dr. T. Kreis (EMBL, Heidelberg, Germany) (23), followed by fluorescein-conjugated affinity-purified goat anti-mouse antibody (Caltag Laboratories, San Francisco). For analysis of polar expression, Caco-2 cells transfected with epitope-tagged SGLT1 grown on permeable supports were fixed and immunostained for the viral epitope using mouse monoclonal antibody P5D4, rabbit polyclonal anti-ZO-1 antiserum (Zymed Laboratories, Inc., S. San Francisco, CA), mouse monoclonal anti-5'-nucleotidase antibody 7G2 (kindly provided by Dr. L. Thompson, Oklahoma Medical Research Foundation, Oklahoma University),<sup>2</sup> or mouse monoclonal antibody against the  $\beta$ -subunit of Na<sup>+</sup>-K<sup>+</sup>-ATPase (kindly provided by Dr. M. Caplan, Department of Physiology, Yale University Medical School). These primarily labeled

<sup>1</sup> The abbreviations used are:  $I_{sc}$ , transepithelial short-circuit current(s);  $\alpha$ MG,  $\alpha$ -methyl glucoside; VSV-G, vesicular stomatitis virus G protein; HBSS, Hanks' balanced saline solution.

<sup>2</sup> G. S. Strohmeyer, S. L. Carlson, L. Thompson, and J. L. Madara, manuscript in preparation.

**FIG. 1. Functional and immunofluorescent detection of epitope-tagged SGLT1 in transiently transfected COS-1 cells.** *A*, transfection increased phloridzin-inhibitable  $\alpha$ MG uptake substantially above that of mock-transfected COS-1 cells. Each bar represents the difference between the mean of two independent measures of  $\alpha$ MG uptake in the absence or presence of phloridzin. *B* and *C*, both surface and intracellular epitope-tagged SGLT1 were detectable by confocal immunofluorescence with the anti-epitope monoclonal antibody (immunofluorescence image (*B*) and phase contrast image (*C*)).



monolayers were then stained with fluorescein-conjugated affinity-purified goat anti-mouse antibody or, for the polyclonal anti-ZO-1 antiserum, fluorescein-conjugated affinity-purified goat anti-rabbit antibody (Cappel). Microscopy was performed using a Zeiss epifluorescence microscope equipped with a Bio-Rad MRC600 confocal unit, computer, and SOM image analysis software.

#### RESULTS

*Transiently Expressed Epitope-tagged SGLT1 Is Immunoreactive, Binds and Internalizes Substrate, and Is Recognized by a Specific Inhibitor*—To avoid disrupting previously described functional regions of SGLT1 (14), we positioned the epitope tag on the C terminus. A commonly used epitope sequence derived from the G protein of vesicular stomatitis virus (23) was used with a short proline-rich spacer between the tag and the C terminus of SGLT1. Transient transfections of epitope-tagged SGLT1 in COS-1 cells demonstrated apparent surface expression of the transfected protein by immunofluorescence (Fig. 1) as well as cytosolic expression within intracellular structures, presumably the endoplasmic reticulum. Surface expression was further documented, as was the functionality of surface epitope-tagged SGLT1, by demonstration of a  $6.9 \pm 0.1$ -fold increase in phloridzin-inhibitable [<sup>14</sup>C] $\alpha$ MG uptake relative to control mock-transfected cells (Fig. 1). Thus, appropriate surface localization, substrate recognition, substrate uptake, and binding of a specific inhibitor were retained by the epitope-tagged construct.

*Kinetic Analysis of Native and Epitope-tagged SGLT1 in Stably Transfected Caco-2 Cells*—Caco-2 cells were stably transfected with either native or epitope-tagged SGLT1, and individual clones were isolated and characterized. Both groups of transfectants displayed marked increases in phloridzin-inhibitable  $\alpha$ MG uptake, thus confirming that transfection of either native or epitope-tagged SGLT1 enhanced Na<sup>+</sup>-sugar cotransport. Clones with high  $\alpha$ MG uptake were selected for examination of steady-state kinetics of  $\alpha$ MG uptake (Fig. 2A). Transport by native SGLT1 demonstrated a dependence on extracellular sugar concentration that fit Michaelis-Menten first-order kinetics,  $J = v_{\max}([S]/([S] + K_m))$ , exhibiting an apparent  $K_m$  of 0.31 mM ( $R^2 = 0.96$ ). This is consistent with the reported  $K_m$  of 0.11 mM for SGLT1 expressed in *Xenopus* oocytes (10). In contrast, the apparent  $K_m$  for  $\alpha$ MG uptake by epitope-tagged SGLT1 was 7.37 mM ( $R^2 = 0.96$ ), representing a 23-fold shift in transport activity. These data indicate that sugar binding and/or transport is disrupted in epitope-tagged SGLT1. As shown in Fig. 1, however, such functionally defined

alterations in the sugar-binding site did not prevent recognition by the specific inhibitor phloridzin, which is thought to also interact with the sugar-binding site (12).

As expected, uptake of  $\alpha$ MG by both native and epitope-tagged SGLT1 was dependent on the extracellular Na<sup>+</sup> concentration (Fig. 2B). The data fit to the Hill equation,  $J = J_{\max} [Na]^n / (K_{Na}^n + [Na]^n)$ , with apparent  $K_{Na}$  values of 43.2 and 69.8 meq/liter for native and epitope-tagged SGLT1, respectively. These data are consistent with the reported value of 32 meq/liter for SGLT1 expressed in *Xenopus* oocytes (10). Hill coefficients of 1.96 and 1.86 were obtained for native SGLT1 ( $R^2 = 0.87$ ) and epitope-tagged SGLT1 ( $R^2 = 0.98$ ), respectively, similar to the reported Hill coefficient for SGLT1 expressed in *Xenopus* oocytes (10). These data are in agreement with previous reports analyzing native SGLT1 and also indicate that, like native SGLT1, epitope-tagged SGLT1 appears to contain two Na<sup>+</sup>-binding sites (6, 27). Thus, in contrast to sugar transport, Na<sup>+</sup> transport appears to be unaffected by the C-terminal epitope tag.

To further evaluate the effect of the epitope tag on sugar transport, the substrate specificities of native and epitope-tagged SGLT1 were compared by competition with similar monosaccharides. The rank order of sugar specificity for both native and epitope-tagged SGLT1 is D-glucose > D-galactose >  $\alpha$ MG > 3-O-methylglucose  $\gg$  L-glucose, mannitol (Fig. 3). This is consistent with previous reports describing sugar specificities for native SGLT1 (10). However, the degrees of inhibition of  $\alpha$ MG uptake by the competing sugars D-glucose, galactose, and 3-O-methylglucose were significantly less with epitope-tagged SGLT1 than with native SGLT1 (Fig. 3). Taken together, these data show that the addition of the epitope tag to the C terminus of SGLT1 alters protein conformation in a subtle yet functionally important fashion.

*The Epitope Tag Is Exposed on the Intracellular Aspect of the Plasma Membrane*—The initial step in Na<sup>+</sup>-sugar cotransport by SGLT1 appears to require extracellular binding of 2 molecules of Na<sup>+</sup> at the luminal surface of the enterocyte (6, 8). While Na<sup>+</sup> transport appears to remain intact, the data indicate that the C-terminal epitope tag may interfere directly with sugar binding. If so, this would imply that the epitope tag (and, by extension, the C terminus of SGLT1) may be exposed on the extracellular face of the membrane. To determine the topology of the epitope tag, antigen accessibility in fixed nonpermeabilized cells was compared with that in fixed permeabilized cells.

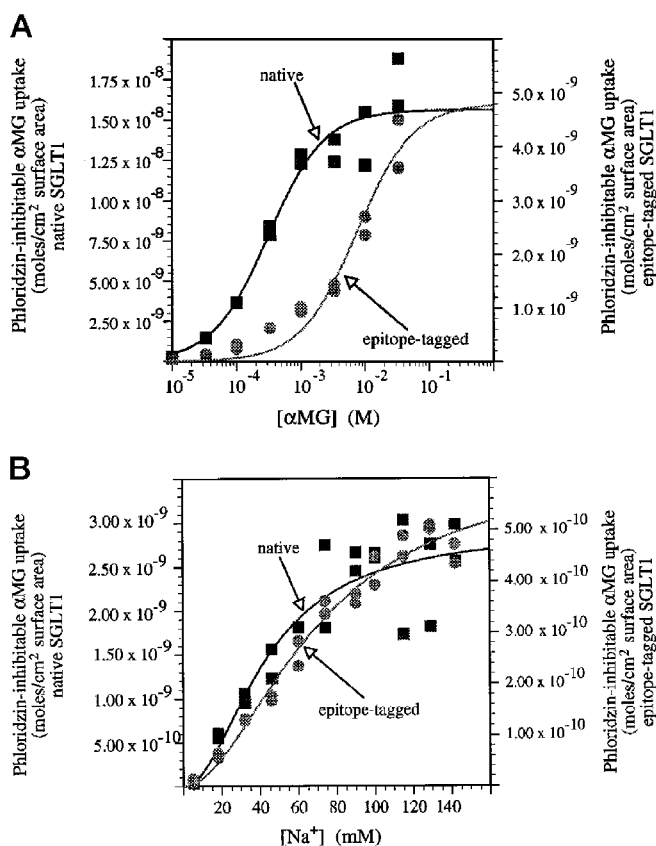


Fig. 2. *A*, first-order kinetics of sugar transport in Caco-2 cells transfected with native or epitope-tagged SGLT1. Shown is the concentration dependence of sugar transport. Native SGLT1 (■) displayed an apparent  $K_m$  of 0.31 mM ( $R^2 = 0.96$ ). In contrast, the apparent  $K_m$  for epitope-tagged SGLT1 (●) was 7.37 mM ( $R^2 = 0.96$ ). Each point represents an individual measurement of  $\alpha$ MG uptake after subtraction of mean nonspecific  $\alpha$ MG uptake, *i.e.* uptake in the presence of phloridzin. Data were fit to Michaelis-Menten first-order kinetics,  $J = v_{\max}([S]/([S] + K_m))$ . *B*, Na<sup>+</sup> dependence of glucose transport in Caco-2 cells transfected with native or epitope-tagged SGLT1. Both native and epitope-tagged SGLT1 display nearly identical dependence on extracellular [Na<sup>+</sup>]. Apparent  $K_{Na}$  values of 43.2 and 69.8 meq/liter were calculated for native SGLT1 (■) and epitope-tagged SGLT1 (●), respectively. Hill coefficients were 1.96 and 1.86 for native SGLT1 ( $R^2 = 0.87$ ) and epitope-tagged SGLT1 ( $R^2 = 0.98$ ), respectively. Each point represents an individual measurement of  $\alpha$ MG uptake after subtraction of mean nonspecific  $\alpha$ MG uptake, *i.e.* uptake in the presence of phloridzin. Data were fit to the Hill equation,  $J = J_{\max}[\text{Na}]^n/([\text{Na}]^n + K_{Na}^n)$ .

Fig. 4 shows that the epitope tag was readily detectable at the cell surface and at intracellular sites in permeabilized cells. In contrast, the epitope tag could not be detected in nonpermeabilized cells. The surface localization of the epitope tag can be confirmed in confocal *xz*-plane images (Fig. 5). These data localize the epitope tag to the intracellular face of the plasma membrane and provide biochemical evidence that the C terminus of SGLT1 is positioned on the cytosolic face of the membrane.

**Trans epithelial Na<sup>+</sup>-Glucose Cotransport by Native and Epitope-tagged SGLT1**—When grown as polarized monolayers on semipermeable supports, stable native SGLT1 transfectants developed moderate transepithelial resistance (Table I, part A), thus affording measurement of SGLT1 function by standard electrophysiologic techniques. In the presence of apical Na<sup>+</sup> and glucose, monolayers of stable native SGLT1 transfectants generated a phloridzin-sensitive current ( $I_{sc}$ ) that was not present in the nontransfected parent line (Table I, part A). Similar  $I_{sc}$  were generated after substitution of  $\alpha$ MG for glucose (data not shown), confirming the ability of the transfected cells to mediate transepithelial Na<sup>+</sup> absorption via apically expressed

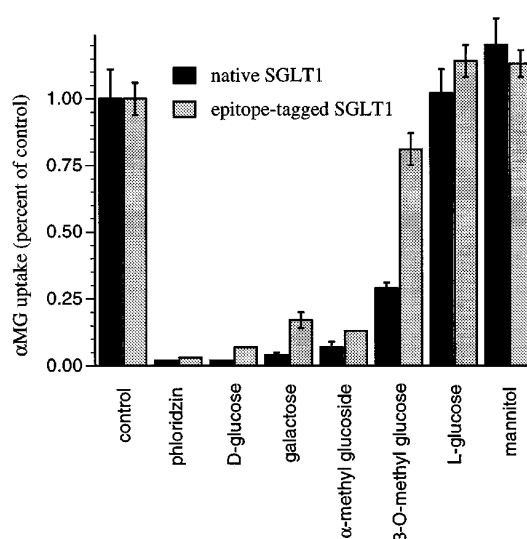
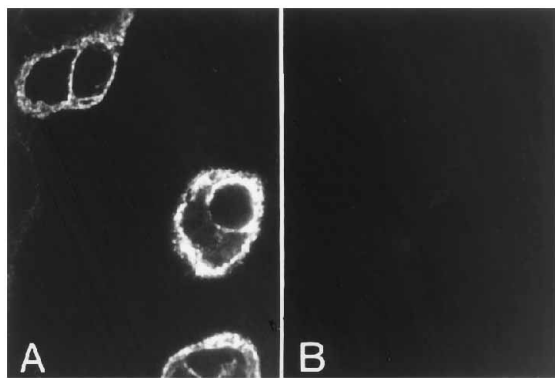


Fig. 3. **Specificity of sugar transport by native and epitope-tagged SGLT1.** To evaluate the substrate specificities of native and epitope-tagged SGLT1, uptake of 100  $\mu$ M  $\alpha$ MG in the presence of 10 mM competing sugar was performed. The concentration of phloridzin was 0.5 mM. Each measurement represents the mean  $\pm$  S.D. of two independent measurements. Data were normalized to uptake in the absence of competing sugars (*Control*).

SGLT1. In contrast, monolayers of stable epitope-tagged SGLT1 transfectants did not possess a phloridzin-inhibitable  $I_{sc}$  (Table I, part A).

**Epitope-tagged SGLT1 Is Not Accurately Targeted to the Apical Membrane**—To determine why the expression of epitope-tagged SGLT1 did not result in Na<sup>+</sup>-glucose cotransport-dependent phloridzin-inhibitable  $I_{sc}$ , the polarity of epitope-tagged SGLT1 expression in monolayers of stable transfectants was examined. Since the generation of  $I_{sc}$  via glucose requires correct targeting of SGLT1 to the apical membrane, expression of a functional Na<sup>+</sup>-glucose cotransporter on the basolateral membrane may lead to phloridzin-inhibitable Na<sup>+</sup>-glucose uptake, but cannot generate transepithelial Na<sup>+</sup> transport. To determine whether missorting of epitope-tagged SGLT1 might, at least in part, explain the loss of  $I_{sc}$ , we examined polarity of epitope-tagged SGLT1 expression by both morphologic and functional methods. Examination of *xz*-plane confocal immunofluorescence images of epitope-tagged SGLT1 in polarized monolayers of epitope-tagged SGLT1 transfectants demonstrated substantial basolateral expression (Fig. 5). To determine whether the loss of selective apical polarization seen with epitope-tagged SGLT1 was unique to the transfected protein or also involved other polarized and selectively targeted proteins, the localizations of the tight junction protein ZO-1, apical 5'-nucleotidase, and basolateral Na<sup>+</sup>-K<sup>+</sup>-ATPase were defined (Fig. 5). In contrast to epitope-tagged SGLT1, all of the latter proteins were correctly sorted to their respective domains, as judged by confocal immunofluorescence microscopy performed on columnar filter-grown monolayers. These data show that missorting is restricted to epitope-tagged SGLT1.

To quantitatively analyze the apical and basolateral expression of epitope-tagged SGLT1 and to directly compare this expression with that of native SGLT1, apical and basolateral phloridzin-inhibitable  $\alpha$ MG uptake were evaluated in polarized monolayers expressing native or epitope-tagged SGLT1 (Fig. 6). Two separate clones transfected independently with native SGLT1 exhibited apically polarized phloridzin-inhibitable uptake. In contrast, two clones transfected independently with epitope-tagged SGLT1 exhibited predominantly basolateral uptake. These functional data provide direct evidence that



**FIG. 4. The epitope tag is localized to the cytoplasmic face of the plasma membrane.** Caco-2 cells transfected with epitope-tagged SGLT1 were grown on coverslips and fixed with paraformaldehyde. Some preparations were then permeabilized with acetone or Triton X-100. Immunostaining for the viral epitope demonstrates inaccessibility of the epitope to extracellular antibody in nonpermeabilized cells (*B*) relative to permeabilized cells (*A*) and verifies that the epitope tag is intracellular (cytoplasmic). Confocal *xy*-plane sections through the mid-portion of the cells are shown. Both surface membrane (also shown in Fig. 5) and cytoplasmic staining are apparent.

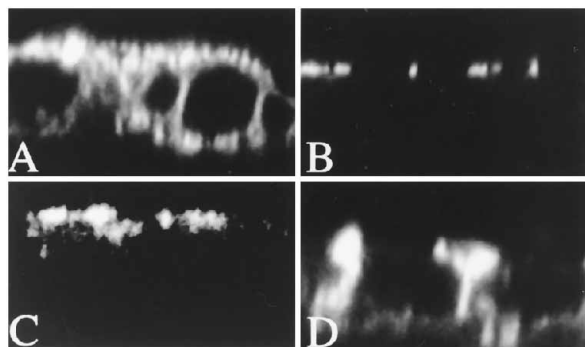


**FIG. 5. Maintenance of apical and basolateral membrane domains in Caco-2 cells transfected with epitope-tagged SGLT1.** Caco-2 cells transfected with epitope-tagged SGLT1 were grown on permeable supports, fixed, permeabilized, and immunostained for the VSV-G epitope tag (*A*), ZO-1 (*B*), 5'-nucleotidase (*C*), or Na<sup>+</sup>-K<sup>+</sup>-ATPase (*D*). Confocal *xz*-plane images are shown.

the VSV-G epitope tag results in disruption of the steady-state distribution of SGLT1 from predominantly apical to predominantly basolateral membrane domains.

Although the majority of epitope-tagged SGLT1 is expressed basolaterally, both functional and morphologic assays show that apical expression still occurs. Nonetheless, a glucose-induced phloridzin-inhibitable  $I_{sc}$  was not detectable. One possibility to explain such data is that apically expressed epitope-tagged SGLT1 is unable to sustain sufficient Na<sup>+</sup> transport to generate a measurable  $I_{sc}$ , perhaps due to the subtle effects of the epitope tag on sugar transport. Alternatively, in the presence of actively transporting basolateral epitope-tagged SGLT1, Na<sup>+</sup> cycling across the basolateral membrane (uptake via basolateral epitope-tagged SGLT1, exit via basolateral Na<sup>+</sup>-K<sup>+</sup>-ATPase) might be substantial enough to interfere with detection of transepithelial Na<sup>+</sup> movement. To differentiate these possibilities, basolateral epitope-tagged SGLT1 was selectively inhibited by the addition of basolateral phloridzin, thus blocking the basolateral Na<sup>+</sup> recycling described above and affording the opportunity to functionally isolate apical epitope-tagged SGLT1. Under these assay conditions, monolayers of epitope-tagged SGLT1 transfectants were able to generate glucose-dependent phloridzin-inhibitable  $I_{sc}$  (Table I, part B). Thus, when basolateral epitope-tagged SGLT1 is inhibited, apical epitope-tagged SGLT1 can initiate phloridzin-inhibit-

able  $I_{sc}$ . These data indicate that epitope-tagged SGLT1, if appropriately polarized, can sustain a transepithelial absorptive Na<sup>+</sup> current despite perturbations in the kinetics of sugar transport.

#### DISCUSSION

The aim of this work was to create an epitope-tagged construct of a polytopic transport protein, SGLT1. Since the C terminus is not highly conserved (9), it seemed a logical location for placement of an epitope tag. Initial studies of epitope-tagged SGLT1 using common approaches confirmed surface expression, global transport function, and sensitivity to specific inhibitors. These data suggested that epitope tagging was successful, and we proceeded with stable transfection into polarized epithelial cells. Studies of stable transfectants showed that, despite the initial characterization, two apparently unrelated functional characteristics of the transporter were disrupted by the epitope tag. These subtle biochemical changes resulted in significant alterations of biologic function.

*The C-terminal Epitope Tag Subtly Alters Transport Characteristics of SGLT1*—Epitope tagging of SGLT1 resulted in an altered apparent  $K_m$  for sugar transport with no effect on the apparent  $K_{Na}$ . Epitope-tagged SGLT1 was also altered in its sensitivity to competing monosaccharides, consistent with an effect on sugar binding, transport, or both. Such an effect might simply be due to disruption of the extracellular glucose-binding site by the foreign sequence. However, our biochemical demonstration that the C-terminal epitope tag is intracellular as well as previous morphologic data showing that antisera against SGLT1 residues 564–575 recognize a cytoplasmic determinant (28) suggest that the C terminus of SGLT1 is cytoplasmic. Thus, it appears most likely that the epitope tag influences glucose transport either by modifying transport across the membrane or by perturbing intracellular release. The epitope tag likely either influences basal conformation or limits conformational changes in SGLT1 associated with substrate binding or translocation. However, the global conformation of SGLT1 does not appear to be perturbed by the epitope tag since transport function is maintained and the apparent  $K_{Na}$  is unaltered.

We initially observed that polarized monolayers of Caco-2 cells transfected with epitope-tagged SGLT1 did not generate phloridzin-inhibitable  $I_{sc}$ . We hypothesized that this might be due to missorting of epitope-tagged SGLT1 and demonstrated both functionally and morphologically that epitope-tagged SGLT1 is missorted. We then sought to verify that missorting, and not the altered  $K_m$ , was responsible for the failure of monolayers expressing epitope-tagged SGLT1 to generate phloridzin-inhibitable  $I_{sc}$ . Monolayers were created with apically polarized expression of epitope-tagged SGLT1 through use of the monolayer-impermeant SGLT1 inhibitor phloridzin. Addition of phloridzin to the basolateral medium selectively inhibited basolateral epitope-tagged SGLT1. Under these conditions, monolayers expressing epitope-tagged SGLT1 were able to generate glucose-dependent  $I_{sc}$  inhibitable by apical phloridzin. This result confirms that missorting, and not altered  $K_m$ , explains the initial inability of epitope-tagged SGLT1 to generate phloridzin-inhibitable  $I_{sc}$ .

*Insights into Potential Relationships between Protein Topology and Transport Function*—As recently reviewed (8), the relationships between SGLT1 sequence, proposed topology, and Na<sup>+</sup>- and glucose-binding sites are likely to be complex. For example, the second and eighth membrane-spanning domains are conserved between a number of homologous Na<sup>+</sup>-coupled solute transporters, the SGLT family, suggesting a central functional role of these sites. A point mutation at Cys-344 (eighth membrane-spanning domain) of the *Escherichia coli* transporter *putP* alters the affinity for Na<sup>+</sup>, pointing to a

TABLE I  
 Transepithelial resistance and glucose-induced  $I_{sc}$  in Caco-2 cells transfected with native and epitope-tagged SGLT1

In part A, Caco-2 cell lines were grown as monolayers on 0.33-cm<sup>2</sup> Transwell inserts. Electrophysiologic readings were taken in apical and basolateral HBSS with 25 mM glucose (the same concentration as in the culture medium). The values after stabilization (<15 min) are shown. The apical medium was then replaced with HBSS with 22.5 mM glucose and 2.5 mM phloridzin. Values after stabilization are reported. Transepithelial resistance in apical and basolateral glucose is shown. In part B, cell growth and electrophysiologic measurements were as described above, except that the basal medium was HBSS with 5 mM glucose, 20 mM mannitol, and 2.5 mM phloridzin.

Caco-2 cell line	$I_{sc}$		SGLT1-mediated $\Delta I_{sc}$	TER <sup>a</sup>
	Apical glucose	Apical phloridzin		
	$\mu A/cm^2$		$\mu A/cm^2$	$Ohm \cdot cm^2$
<b>A. Electrophysiology under standard assay conditions</b>				
Parent	-1.1 ± 0.3	-0.9 ± 0.0	0.2 ± 0.3	224 ± 1
Native clone 1	-4.3 ± 0.2	-3.2 ± 0.4	1.1 ± 0.4	162 ± 19
Native clone 2	-4.9 ± 0.6	-3.3 ± 0.3	1.6 ± 0.7	168 ± 20
Epitope-tagged clone 1	-1.6 ± 0.2	-2.4 ± 0.1	-0.8 ± 0.2	241 ± 7
Epitope-tagged clone 2	-1.6 ± 0.2	-2.0 ± 0.3	-0.4 ± 0.4	375 ± 58
<b>B. Electrophysiology with basolateral phloridzin</b>				
Epitope-tagged clone 1	-3.6 ± 0.1	-2.4 ± 0.1	1.2 ± 0.1	
Epitope-tagged clone 2	-2.5 ± 0.5	-2.0 ± 0.3	0.5 ± 0.6	

<sup>a</sup> TER, transepithelial resistance.

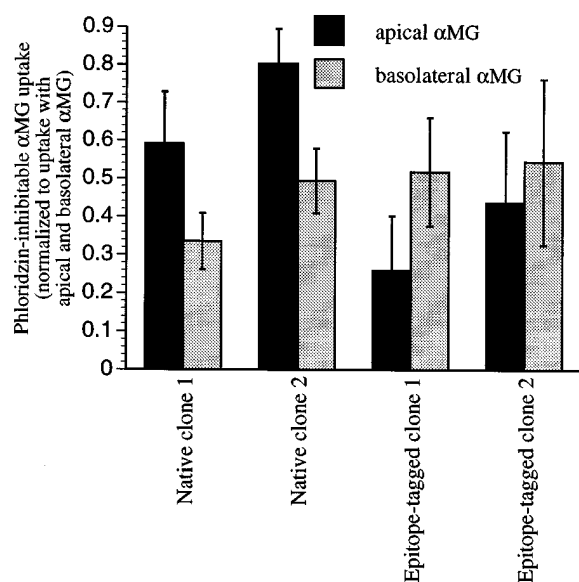


FIG. 6. **Polarity of SGLT1-mediated sugar transport in Caco-2 cells transfected with native or epitope-tagged SGLT1.** To evaluate the polarity of functional SGLT1 expression, transfected cells were grown on permeable supports. Uptake of  $\alpha$ MG was measured following incubation with apical, basolateral, or apical and basolateral  $\alpha$ MG. Uptake of  $\alpha$ MG in the presence of phloridzin was also measured under each of these conditions. Phloridzin-inhibitable uptake of  $\alpha$ MG applied only to the apical or basolateral surface was normalized to phloridzin-inhibitable uptake of  $\alpha$ MG applied to apical and basolateral surfaces. Data are the means  $\pm$  S.D. of two monolayers for each condition.

role for this domain in Na<sup>+</sup> binding (29). However, a point mutation at Gly-22 (first membrane-spanning domain) in *putP* has a similar effect on the affinity for Na<sup>+</sup> (30), and a mutation at Arg-257 (within the cytoplasmic loop that separates the sixth and seventh membrane-spanning domains) eliminated the Na<sup>+</sup> dependence of solute binding (31). Such observations are consistent with the hypothesis that several distinct elements within the primary structure of SGLT family members, including SGLT1, influence the tertiary structure that forms the Na<sup>+</sup>-binding site (8).

On the basis of sequence homology, sites including the extracellular loop that separates the third and fourth membrane-spanning domains, membrane-spanning region 5, and the segment between membrane-spanning regions 9 and 11 have been suggested as possibly involved in solute, *e.g.* glucose, binding (8). In contrast, the current studies suggest that modifications of the C terminus influence both the kinetics and hierarchy of

sugar binding, without affecting the kinetics or stoichiometry of Na<sup>+</sup> binding. These observations indicate that the tertiary structure that determines sugar transport can be influenced independently of the Na<sup>+</sup>-binding site and raise the possibility that determinants of the sugar transport site may reside preferentially in the C terminus, while those determining Na<sup>+</sup> binding may reside preferentially in an extended N-terminal domain.

**Disruption of Apically Polarized SGLT1 Expression by Epitope Tagging**—The sorting of epitope-tagged SGLT1 to the basolateral surface may be due to the basolateral targeting sequence present within the cytoplasmic tail of VSV-G. A portion of this sequence is included in the epitope tag, which is composed of residues 19–29 of the cytoplasmic tail of VSV-G. Characterization of this targeting signal has identified Tyr-19 and Ile-22 as the most critical residues for basolateral targeting, with Arg-16 playing a minor role (32). When residues 14–29 of the cytoplasmic tail of VSV-G replace the cytoplasmic tail of the normally apical influenza hemagglutinin protein, 58% of the fusion protein is delivered basolaterally (32). In addition to consensus primary sequences, some data suggest that a type I  $\beta$ -turn is critical for basolateral targeting (32–34). In fact, it may be that the presence of Arg-16 facilitates this conformation. Our use of only residues 19–29 of the cytoplasmic tail of VSV-G and an 8-residue proline-rich sequence to ensure separation of the VSV-G epitope from the membrane (models of the C terminus of SGLT1 differ in length and topology of the C-terminal extramembranous extension) makes it unlikely that the VSV-G sequence could adopt a  $\beta$ -turn conformation. Thus, the data from epitope-tagged SGLT1 suggest that a type I  $\beta$ -turn may not be absolutely required for basolateral targeting by the VSV-G sequence.

The basolateral targeting sequences characterized to date are all derived from monotopic proteins (32–36). Assays characterizing these sequences have also depended on monotopic proteins, *e.g.* hemagglutinin. Thus, the ability of these sequences to accurately target polytopic proteins has not been previously analyzed. Our data demonstrating the ability of the VSV-G sequence to target SGLT1 to the basolateral membrane show that basolateral targeting sequences from monotopic proteins can direct targeting of polytopic proteins. Furthermore, since the full-length SGLT1 protein is present within the epitope-tagged construct, the data also show that the VSV-G basolateral sequence is dominant over endogenous apical targeting information. The identity of endogenous apical targeting information within SGLT1 is not known. It is possible that the SGLT1 apical targeting information is contained within an

extracellular (luminal) domain, as has been suggested for dipeptidyl peptidase IV (35).

**Caveats to Epitope Tagging**—Clearly, the method of epitope tagging is useful since it provides a means to mark specific molecules for which specific high quality reagents, *e.g.* monoclonal antibodies, are not available. However, given the increasing use of epitope tagging, the data presented must be taken as a cautionary note. This may be particularly true for membrane proteins, especially polytopic ones. Despite preliminary studies in nonpolarized and polarized cells that suggested that global function was intact in epitope-tagged SGLT1, function was clearly altered in several distinct ways. Thus, characterization of transport kinetics, substrate specificities, and polarity of expression was critical to adequately document the multiple functions disrupted by the epitope tag. Unfortunately, these types of sensitive assays are not available for many molecules. Thus, the results stress the need for careful evaluation of epitope-tagged membrane proteins.

**Acknowledgments**—We thank Drs. Daniel Louvard, Monique Arpin, and Sylvie Robine for many helpful interactions during the initiation of this project and for review of the manuscript. We also thank Drs. Randy Mrsny, Ernest Wright, and Mathias Hediger for helpful discussions; Drs. Ernest Wright, Mark Mooseker, Thomas Kreis, Michael Caplan, and Linda Thompson for providing valuable reagents; and Dr. Tucker Collins for advice and support in initial confirmation of the nature of the SGLT1 cDNA.

#### REFERENCES

- Geli, V., Baty, D., and Lazdunski, C. (1988) *Proc. Natl. Acad. Sci. U. S. A.* **85**, 689–693
- Meichsner, M., Doll, T., Reddy, D., Weisshaar, B., and Matus, A. (1993) *Neuroscience* **54**, 873–880
- Algrain, M., Turunen, O., Vaheri, A., Louvard, D., and Arpin, M. (1993) *J. Cell Biol.* **120**, 129–139
- Wadzinski, B. E., Eisfelder, B. J., Peruski, L. F., Jr., Mumby, M. C., and Johnson, G. L. (1992) *J. Biol. Chem.* **267**, 16883–16888
- Ellison, M. J., and Hochstrasser, M. (1991) *J. Biol. Chem.* **266**, 21150–21157
- Wright, E. M. (1993) *Annu. Rev. Physiol.* **55**, 575–589
- Hediger, M. A., Coady, M. J., Ikeda, T. S., and Wright, E. M. (1987) *Nature* **330**, 379–381
- Hediger, M. A., and Rhoads, D. B. (1994) *Physiol. Rev.* **74**, 993–1026
- Wright, E. M., Loo, D. D., Panayotova-Heiermann, M., Lostao, M. P., Hirayama, B. H., Mackenzie, B., Boorer, K., and Zampighi, G. (1994) *J. Exp. Biol.* **196**, 197–212
- Ikeda, T. S., Hwang, E.-S., Coady, M. J., Hirayama, B. A., Hediger, M. A., and Wright, E. M. (1989) *J. Membr. Biol.* **110**, 87–95
- Kimmich, G. A., and Randles, J. (1981) *Am. J. Physiol.* **241**, C227–C232
- Toggenburger, G., Kessler, M., and Semenza, G. (1982) *Biochim. Biophys. Acta.* **688**, 557–571
- Lee, W. S., Kanai, Y., Wells, R. G., and Hediger, M. A. (1994) *J. Biol. Chem.* **269**, 12032–12039
- Turk, E., Zabel, B., Mundlos, S., Dyer, J., and Wright, E. M. (1991) *Nature* **350**, 354–356
- Turk, E., Martin, M. G., and Wright, E. M. (1994) *J. Biol. Chem.* **269**, 15204–15209
- Le Bivic, A., Quaroni, A., Nichols, B., and Rodriguez-Boulant, E. (1990) *J. Cell Biol.* **111**, 1351–1361
- Peterson, M. D., Bement, W. M., and Mooseker, M. S. (1993) *J. Cell Sci.* **105**, 461–472
- Peterson, M. D., and Mooseker, M. S. (1993) *J. Cell Sci.* **105**, 445–460
- Pinto, M., Robine-Leon, S., Appay, M. D., Keding, M., Triadou, N., Dussaulx, E., Lacroix, B., Simon-Assmann, P., Haffen, K., Fogh, J., and Zweibaum, A. (1983) *Biol. Cell* **47**, 323–330
- Matter, K., Brauchbar, M., Bucher, K., and Hauri, H. P. (1990) *Cell* **60**, 429–437
- MacDonald, R. S., Thornton, W. H., Jr., and Bean, T. L. (1993) *J. Recept. Res.* **13**, 1093–1113
- Riley, S. A., Warhurst, G., Crowe, P. T., and Turnberg, L. A. (1991) *Biochim. Biophys. Acta* **1066**, 175–182
- Kreis, T. E. (1986) *EMBO J.* **5**, 931–941
- Brewer, C. B., and Roth, M. G. (1991) *J. Cell Biol.* **114**, 413–421
- Peterson, M. D., and Mooseker, M. S. (1992) *J. Cell Sci.* **102**, 581–600
- Madara, J. L., and Stafford, J. (1989) *J. Clin. Invest.* **83**, 724–727
- Brot-Laroche, E., Supplisson, S., Delhomme, B., Alcalde, A. L., and Alvarado, F. (1987) *Biochim. Biophys. Acta* **904**, 71–80
- Takata, K., Kasahara, T., Kasahara, M., Ezaki, O., and Hirano, H. (1992) *Cell Tissue Res.* **267**, 3–9
- Hanada, K., Yoshida, T., Yamato, I., and Anraku, Y. (1992) *Biochim. Biophys. Acta* **1105**, 61–66
- Yamato, I., Ohsawa, M., and Anraku, Y. (1990) *J. Biol. Chem.* **265**, 2450–2455
- Ohsawa, M., Mogi, T., Yamamoto, H., Yamato, I., and Anraku, Y. (1988) *J. Bacteriol.* **170**, 5185–5191
- Thomas, D. C., and Roth, M. G. (1994) *J. Biol. Chem.* **269**, 15732–15739
- Hunziker, W., Harter, C., Matter, K., and Mellman, I. (1991) *Cell* **66**, 907–920
- Aroeti, B., Kosen, P. A., Kuntz, I. D., Cohen, F. E., and Mostov, K. E. (1993) *J. Cell Biol.* **123**, 1149–1160
- Weisz, O. A., Machamer, C. E., and Hubbard, A. L. (1992) *J. Biol. Chem.* **267**, 22282–22288
- Monlauzeur, L., Rajasekaran, A., Chao, M., Rodriguez-Boulant, E., and Le Bivic, A. (1995) *J. Biol. Chem.* **270**, 12219–12225